Space Sci Rev (2017) 206:407–429
DOI 10.1007/s11214-016-0320-x

Post-Storm Middle and Low-Latitude Ionospheric Electric Fields Effects

B.G. Fejer[1] · M. Blanc[2] · A.D. Richmond[3]

Received: 11 March 2016 / Accepted: 21 November 2016 / Published online: 5 December 2016

Abstract The Earth's upper atmosphere and ionosphere undergoes large and complex perturbations during and after geomagnetic storms. Thermospheric winds driven by enhanced energy and momentum due to geomagnetic activity generate large disturbance electric fields, plasma drifts and currents with a broad range of temporal and spatial scales from high to equatorial latitudes. This disturbance dynamo mechanism plays a fundamental role on the response of the middle and low-latitude ionosphere to geomagnetic activity. In this review, we initially describe the early evidence for the importance of this process and the first simulation study which already was able to explain its main effects on the electrodynamics of the middle and low-latitude ionosphere. We then describe the results of more recent simulations and the extensive experimental work that highlights the importance of this mechanism for ionospheric space weather studies extending to post-storms periods, and present some suggestions for future studies.

Keywords Electric fields · Ionospheric dynamics · Ionospheric storms · Ionosphere/atmosphere interactions

1 Introduction

Electric fields and neutral winds play fundamental roles on the dynamics and energetics of the upper atmosphere and on the plasma density and composition of the ionosphere. Quiet-time ionospheric electric fields and currents are generated mostly by the dynamo action of tides and thermospheric winds driven by solar heating and lunar gravitational effects (e.g., Richmond 1995). The general characteristics of middle and low-latitude quiet-time electrodynamic E × B plasma drifts were described in numerous publications (e.g., Kelley 1988; Fejer 1997).

✉ B.G. Fejer
bela.fejer@usu.edu

1 Center for Atmospheric and Space Sciences, Utah State University, Logan, UT 84322-4405, USA

2 IRAP/Observatoire Midi-Pyrénées, UPS, 31028 Toulouse Cedex 4, France

3 NCAR-HAO, P.O. Box 3000, Boulder, CO 80307-3000, USA

Geomagnetic activity has long been known to cause complex large-scale ionospheric electrodynamic disturbances from high to equatorial latitudes (e.g., Matsushita 1953; Rastogi 1962; Nishida et al. 1966). Over the last several decades, middle and low-latitude storm-time electric fields and currents have been studied extensively using ground-based and satellite measurements, and global convection and general circulation models (e.g., Blanc 1978; Kelley et al. 1979; Gonzales et al. 1979; Blanc and Richmond 1980; Blanc 1983a, 1983b; Senior and Blanc 1984; Mazaudier et al. 1987; Spiro et al. 1988; Fejer et al. 1991; 1990; 2007; Fejer 2002; Peymirat et al. 2000, 2002; Richmond et al. 2003; Maruyama et al. 2005, 2007; Abdu et al. 2007; Huang et al. 2007, 2010; Kikuchi et al. 2008; Wei et al. 2008, 2011; Veenadhari et al. 2010). Storm-time electric fields and currents cover a broad range of temporal scales and vary with local time, season, solar flux, latitude, and longitude. At subauroral and upper middle latitudes, magnetic storms often generate very large (up to about 100 mV/m) and highly structured polarization electric fields, which drive highly structured plasma density enhancements extending to the outer plasmasphere (e.g., Foster et al. 2002). In the low and equatorial regions, storm-time zonal electric fields drive vertical disturbance drifts that can strongly affect ionospheric plasma density distributions and the generation and evolution of equatorial plasma waves and structures with a large range of scale sizes (e.g., Fejer 2011).

In the 1970s and 1980s, observational evidence and theoretical studies progressively established that two concurrent dynamo sources are needed to explain the spatial distribution and temporal variability of storm-time middle and low-latitude ionospheric electric field and current disturbances: the solar-wind/magnetospheric dynamo, and the ionospheric disturbance dynamo. The solar-wind/magnetospheric dynamo generates large global electrodynamic perturbations extending nearly simultaneously down to the mid-latitudes (Blanc 1978; Blanc 1983a, 1983b) and to the equator during periods of strong geomagnetic activity (e.g., Kelley et al. 1979; Abdu et al. 2007). These so-called prompt penetration electric fields and currents are usually short-lived (time scales from a few minutes to a few hours), but can be longer lasting during extended continuous periods of strong geomagnetic activity (e.g., Maruyama et al. 2007; Wei et al. 2008; Huang 2015). They occur most strongly after large and sudden changes in the high-latitude convection, before the plasma sheet inner edge and the region-2 field-aligned currents have had time to reconfigure so as to counteract the convection of plasma between the outer and inner magnetosphere, thereby counteracting the penetration of electric fields to lower latitudes and producing steady-state shielding. Undershielding occurs after a rapid increase in magnetospheric convection, when polar-cap convection penetrates directly to middle and low-latitudes, while overshielding occurs after a rapid decrease in magnetospheric convection, when the electric fields associated with region-2 currents initially overcompensate the directly penetrating fields (Wolf 1983; Senior and Blanc 1984; Spiro et al. 1988; Peymirat et al. 2000). The ionospheric disturbance dynamo, on the other hand, generates global middle and low-latitude electrodynamic disturbances due to the dynamo action of equatorward propagating neutral wind surges and circulation changes driven by enhanced energy and momentum deposition into the high-latitude ionosphere during geomagnetically disturbed times (e.g., Blanc and Richmond 1980; Fuller-Rowell et al. 2002). These perturbations can appear at the equator within about 1–3 hours, have typical time scales of several hours, and can last up to 1–2 days after geomagnetic activity has subsided (e.g., Scherliess and Fejer 1997; Kumar et al. 2010).

Two main pieces of evidence were found in favor of the simultaneous existence and comparable importance of the current and field disturbances produced by these two dynamos at low and middle-latitudes.

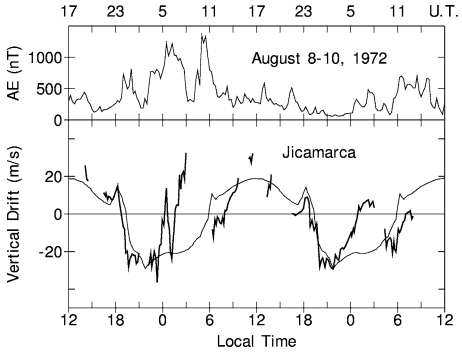

Fig. 1 Equatorial F-region vertical plasma drifts and auroral electrojet indices during a two-day period of strong geomagnetic activity. The *thin curve* corresponds to the average quiet-time pattern (after Scherliess and Fejer 1997)

First, their effects can sometimes be clearly separated in time: let us take a particularly clear example of that from an equatorial observation. Figure 1 shows equatorial F-region vertical plasma drifts measured at the Jicamarca Radio Observatory (11.9°S, 76.8°W; dip latitude 1°N), near Lima, Peru, during the large geomagnetic storm of 8–10 August 1972. Over Jicamarca an upward drift velocity of 40 m/s corresponds to an eastward electric field of about 1 mV/m. The large short-lived vertical drift perturbations between about 04 and 08 UT on 9 August are likely due to the prompt penetration of magnetospheric zonal electric fields into the equatorial ionosphere, since they occur simultaneously with the high-latitude disturbance. These equatorial prompt penetration vertical drifts are upward (downward) during daytime undershielding (overshielding) conditions, and have opposite direction at night. Figure 1 also shows large longer-lived nighttime upward perturbation drifts between about 02 and 08 UT on the following night. These more slowly varying upward perturbation drifts, which have a direction opposite to the quiet-time vertical drifts, could not be driven by the solar-wind/magnetospheric dynamo, since they occurred when geomagnetic activity had largely quieted down: they were likely driven by ionospheric disturbance dynamo electric fields (Scherliess and Fejer 1997), which are the focus of this work. However, prompt penetration and disturbance dynamo processes often occur simultaneously and can interact with each other, especially during long lasting magnetic storms, when prompt penetration effects can modify nighttime disturbance dynamo electric fields (e.g., Maruyama et al. 2005). This frequently makes the distinction of the electrodynamic disturbances from the two dynamos difficult.

But another piece of evidence in favor of the superposition of the two dynamos, less sensitive to the simultaneity problem, was provided by a specific feature of the zonal disturbance electrodynamic drifts observed in the mid-latitude F-region by the Saint-Santin (L = 1.8, geomagnetic latitude 47°) radar (Blanc 1978; Blanc 1983a) during periods of strong geomagnetic activity: analysis of its data (Fig. 2) showed the dominance of moderate to strong westward drifts at essentially all local times. This trend could be observed both during an individual long-lasting magnetic storm (top panel), and when averaging over all periods of strong magnetic disturbances (bottom panel). In addition to this dominant westward drift, a diurnal variation of similar amplitude is also clearly seen in the data. The conjunction of these two features strongly suggested that the observed drift pattern could result from the superposition of direct penetration effects due to the solar-wind/magnetospheric dynamo, producing their local-time variation, with disturbance dynamo effects producing an additional westward drift of the F-region plasma at all local times, as first noticed by Blanc and Richmond in their 1980 study of the disturbance dynamo which will be described later.

In the following sections, we first examine the causes and electrodynamic effects of the disturbance dynamo mechanism, as analyzed by Blanc and Richmond (1980) and by later

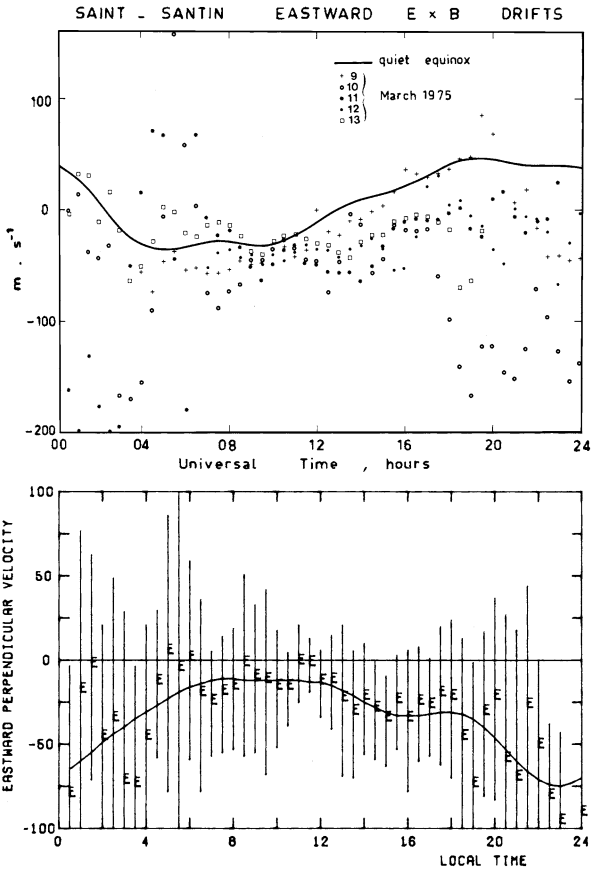

Fig. 2 Zonal E × B F-region plasma drifts measured with the Saint-Santin tristatic incoherent scatter radar: (*top*) data points show all zonal drifts measured during 5 days of the magnetic storm of March 9, 1975. Observed storm-time drifts are systematically westwards of the average quiet-time reference (*full curve*), with maximum departures during night-time. (*Bottom*) The same trend remains when all disturbed time drift data are averaged through the whole Saint-Santin data set. The figure shows the average (E) and data set dispersion (*vertical bars*) of all disturbance drifts (e.g. differences between data and average for quiet days) as a function of local time. The *vertical bars* indicate the variability of the residuals and not the error bars of the measurements, which are much smaller (after Blanc 1983a)

complementary studies. We then describe the characteristics of observed low- and mid-latitude disturbance dynamo electric fields derived from ionospheric plasma drift and current measurements, focusing on post-storm conditions. Finally, in light of a comparison of the more and more sophisticated model predictions with the accumulating body of observations, we discuss current outstanding efforts towards improving our understanding of post-storm middle and low-latitude ionospheric electrodynamics, and we suggest possible directions for future progress.

2 The Ionospheric Disturbance Dynamo

The first theoretical description and modeling of the ionospheric disturbance dynamo was published by Blanc and Richmond in 1980. That study was motivated mainly by two considerations.

First, as had been noted by Volland and Mayr 1971; Testud et al. 1975, and Blanc 1978; Blanc and Richmond 1980 recognized that the energy deposition into the thermosphere at high-latitudes associated with magnetic storms, even as poorly evaluated as it was at the time, was important enough to produce significant disturbances of the neutral wind field and of the associated electrodynamic parameters down to the equator: so, a "disturbance dynamo" of some kind just had to exist.

Second, they were well aware of a set of middle and low-latitude observations that could not be explained solely by solar-wind/magnetosphere dynamo effects. This was particularly the case for two features we already illustrated in our introduction:

- **feature 1**: westward departure of the E × B F-region drifts from their quiet-time values are observed at all local times near 45 degrees midlatitude (see Fig. 2);
- **feature 2**: magnetic-storm associated disturbances in vertical E × B drifts are observed at the magnetic equator for a long time into the recovery phase, when magnetic activity has quieted down (see Fig. 1).

Thus, starting from their knowledge of the sources of auroral heating, they developed a theoretical model which essentially used these sources to set the thermosphere into motion and produce a disturbed wind field, and to calculate the electrodynamic parameter disturbances produced by the dynamo action of these fields.

Neutral Wind Response to Auroral Heating The first step was to calculate the neutral wind field produced by auroral heating during storms. They reduced their heating source to Joule heating, because the other significant source, particle precipitation heating, though sometimes of a comparable magnitude, deposits energy at a much lower altitude, in a significantly denser atmosphere which could not be so easily set into motion. They used in their calculation the zonally symmetric, time dependent, thermospheric dynamics model of Richmond and Matsushita (1975). The use of a zonally symmetric thermosphere dynamics model had the following justification:

- zonally symmetric circulation is usually the dominant mode, and the easiest to set-up and maintain, in a rotating atmosphere, and it is expected to prevail even in response to an asymmetric high-latitude heat input;
- consequences of this restriction were to be partially checked, at the end of the study, by using different wind systems artificially confined to the dayside or to the nightside;
- finally, this zonal symmetry of assumed neutral winds was partly compensated by the parallel consideration of two different descriptions of background ionospheric parameters: a first one representative of the nightside (case I), and a second one more representative of the dayside (case II). Given the amount of global Joule heating assumed in each case, case I was considered as representative of a strong magnetic storm, while case II was considered as representative of weak magnetic activity, and perhaps even of quiet times.

Results of these simulations, in which a long-lasting heating of the auroral thermosphere is imposed, immediately showed that (for case I) strong disturbed winds were generated nearly down to the equator above the altitude of maximum heating (about 120 km). While meridional winds displayed all the features of a giant Hadley cell driven by the auroral heat source (with updrafts above the heating source, horizontal equatorward winds, and downdrafts at low-latitudes), strong westward zonal winds built up from subauroral to equatorial latitudes, thus producing a sub-corotation of the thermosphere which was the signature of angular momentum transfer from auroral to lower latitudes.

Prediction of the Electrodynamic Disturbances: (1) Zonally Symmetric Dynamo Model A zonally symmetric ionospheric dynamo model was first used to generate electrodynamic parameters. In such a simple model, zonal symmetry and the irrotational nature of the electrostatic field impose that the zonal electric field component is null. Hence the electric field is purely meridional, and the E × B drift that it drives is purely zonal. Despite this limitation, model results proved capable of capturing a good fraction of the features of the disturbance dynamo:

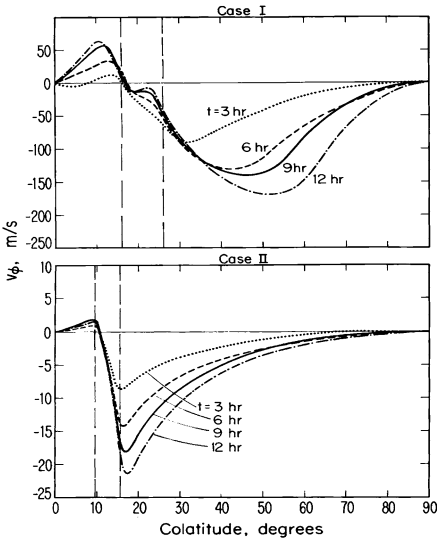

Fig. 3 Latitudinal variation of the E × B F-region plasma drifts for different times in the simulated storm development, and for the two simulation cases (I at the top and II at the bottom). Build-up of strong westward drifts all over midlatitudes appears particularly clearly for case I, which corresponds to a strong storm (after Blanc and Richmond 1980)

– The essentially equatorward and westward neutral winds generated above 120 km both contribute to drive an equatorward electric current flow down to the equator.
– Consequently, the equatorial regions accumulate positive charges, thereby inducing in return a poleward electric field and a strong eastward Hall current flowing all around the globe. This poleward electric field also drives strong westward E × B drifts all over midlatitudes, producing a subrotation of the F-region plasma, and actually also of the whole region of the plasmasphere electrically connected to it by near-equipotential magnetic field lines.

Thus **feature 1** is already reproduced in this simplified zonally symmetric approach. Figure 3 shows the spectacular build-up of these westward drifts as a function of increasing storm time for the two simulation cases, I and II. Notice that the westward drift for the weaker disturbance (case II) increases steadily with time for the first 12 hours, while that for the stronger disturbance (case I) tends to saturate after several hours at the higher latitudes, owing to the nonlinear dynamics of the thermosphere. As expected, westward drift disturbances reach significantly lower latitudes for case I than for case II.

Prediction of the Electrodynamic Disturbances: (2) a More Realistic Dynamo Model
Since no zonal electric field (and therefore vertical plasma drift) can be generated in a zonally symmetric dynamo model, reproduction of feature 2 required a more sophisticated model breaking zonal symmetry. To achieve this, Blanc and Richmond used a full 3-D numerical dynamo model, in which however they kept the same zonally symmetric wind fields, but introduced realistic spatial distributions of the height-integrated ionospheric conductivities. Since one of the challenges was to correctly reproduce the equatorial electrodynamic parameters, they introduced an original description of the low-latitude boundary condition connecting the planetary ionospheric conducting shell to the equatorial electrojet region: the whole electrojet region between $+10°$ and $-10°$ magnetic latitude was represented as a "thin wire", the total electrojet current was modeled as directly proportional to the zonal electric field, and current continuity between electrojet and planetary currents was assumed across the boundary. At high-latitudes they assumed perfect steady-state shielding of the

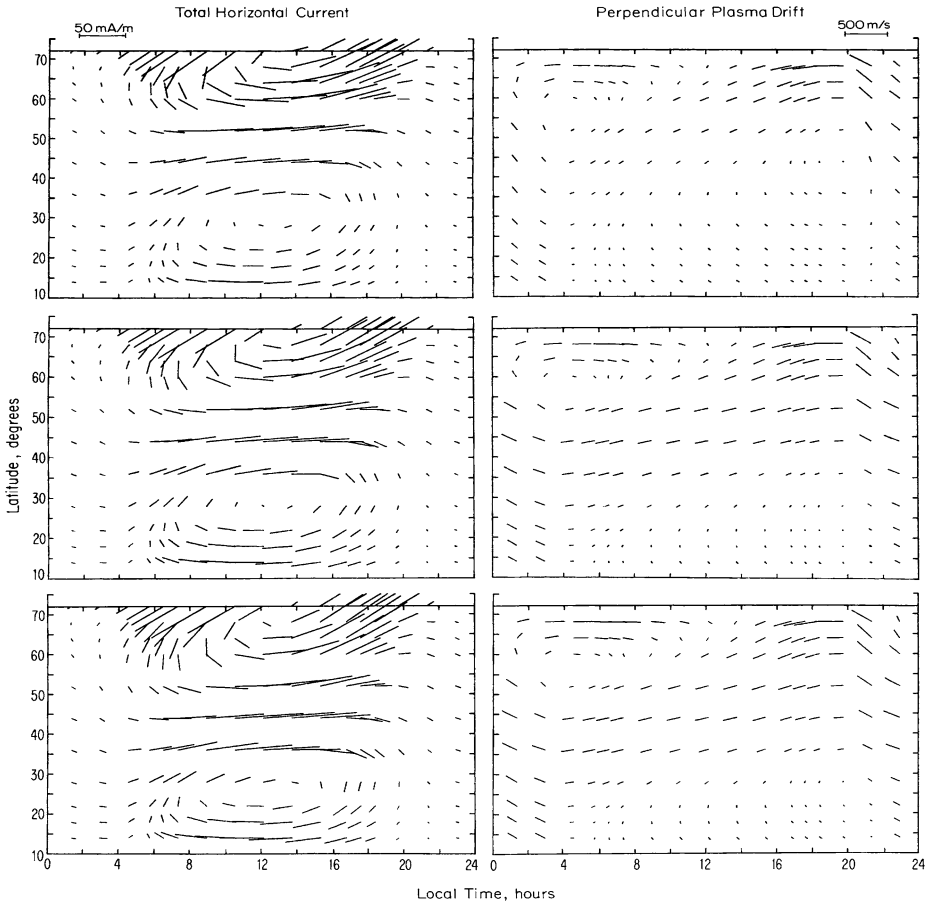

Fig. 4 Hemispheric distribution of the total horizontal currents (*left panels*) and of the E × B F-region plasma drifts, calculated for three different times into storm development (3, 6 and 9 hours) and for case I (after Blanc and Richmond 1980)

middle- and low-latitude regions from the magnetospheric dynamo by setting the electric potential to a constant value at 72° latitude.

Results of this simulation for case I (strong storm) are displayed in Fig. 4 in terms of the hemispheric distributions of height-integrated electric currents (left-hand panels) and F-region E × B drifts (right-hand panels) for three times after the onset of auroral heating (3, 6 and 9 hours).

The first thing we note is that feature 1 is still present at high enough latitudes (above 35°). But in addition, a new interesting electrodynamic behavior appears: the strong eastward current flow observed in the zonally symmetric dynamo calculation is still present and dominant on the dayside, roughly between 35 and 55° latitude. But it is now interrupted, and diverted poleward and equatorward, by the strong conductivity gradients at the dawn and dusk terminators. The diverted currents close via two vortices which form poleward and equatorward of the strong eastward current flow region.

The equatorward vortex resembles an "anti-Sq" current system, flowing essentially opposite to the quiet-day currents and therefore counter-balancing them. It closes through the

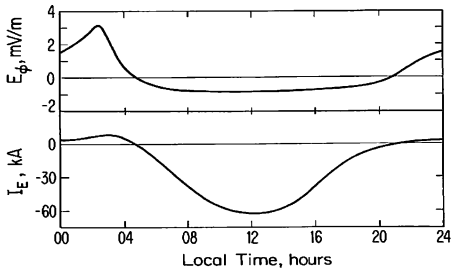

Fig. 5 Local time distributions of the two main electrodynamic parameters of the equatorial ionosphere, the eastward electric field and the total eastward electric current in the electrojet region integrated between $+10°$ and $-10°$ latitude, predicted by the case I simulation. Both parameter variations are basically reversed from their observed quiet-day variations (after Blanc and Richmond 1980)

equatorial electrojet, flowing westward on the dayside, and eastward on the nightside, just opposite to the regular electrojet flow. The resulting equatorial electrodynamic parameters local time variation is shown in Fig. 5. Both the eastward electric field (inducing the vertical $E \times B$ plasma drift) shown in the top panel, and the total electrojet current shown in the bottom panel, display variations opposite to their quiet-day behavior: globally, a dusk-to-dawn electrostatic potential drop is generated, inducing westward currents and downward plasma drifts on the dayside, and just opposite on the nightside. This behavior also results in the weakening of the equatorial anomaly usually produced by the equatorial plasma fountain. As one observes, **feature 2** is thus also reproduced by this more sophisticated dynamo model.

As a final check, Blanc and Richmond partly tested the sensitivity of their model results to the most restrictive assumption, the use of zonally symmetric neutral winds, by performing two additional simulations in which the wind system was confined either to the dayside, or to the nightside. They found that the dayside winds alone are the more effective in generating the global dynamo fields and currents, in that they generate a distribution of these quantities which is qualitatively similar to the predictions shown in Fig. 4, obtained with the zonally symmetric winds. On the other hand, the electrodynamic electric field effects of the nightside winds are essentially confined to the night side, where at midlatitudes they create poleward electric fields, and at low-latitudes they create westward evening fields and eastward early-morning fields.

Main Lessons Learnt from the Blanc-Richmond Study Despite the limited data sets available at the time to validate their predictions, this early theoretical formulation and study of the ionospheric disturbance dynamo was able to reproduce two of the most intriguing observed features of low- and middle-latitude electrodynamic parameters during magnetic disturbance periods, previously called features 1 and 2, which the solar-wind/magnetospheric dynamo alone was unable to reproduce. This result provided the first strong support to the very existence of the ionospheric disturbance dynamo, and established its main morphological features on a theoretical basis for the different latitude regions. Further studies were to refine and deepen these two points.

Further Studies The first issue to be addressed in the years following the Blanc-Richmond study was the difficult question of the separation of the combined effects of the solar-wind/magnetospheric and ionospheric disturbance dynamos in real data. Blanc (1983b) showed that it was possible to disentangle the two contributions in Saint-Santin

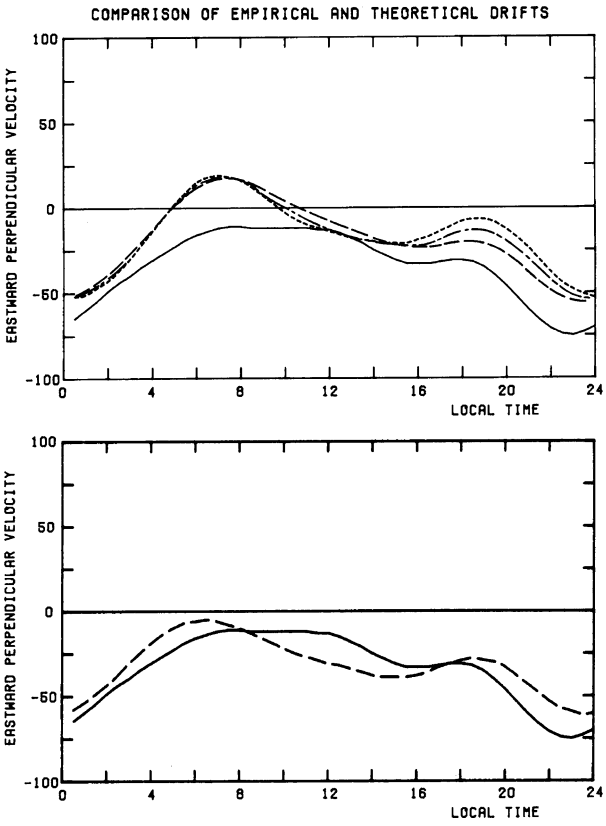

Fig. 6 Comparison of the local time variation of the average eastward disturbance F-region E × B drifts above Saint-Santin (*continuous curve*, also reproducing the *full curve* on the bottom panel of Figure 2) with predictions of the effects of the two dynamos. *Top panel*: solar-wind/magnetospheric dynamo effects only (for Hall-to-Pedersen height-integrated conductivity ratios of 1.3, 1.7 and 2); *bottom panel*: with addition of the effects of the ionospheric disturbance dynamo. It is the superposition of the effects of the two dynamos which allows a satisfactory reproduction of the observed drifts (after Blanc 1983b)

zonal F-region plasma drift data, which are dominated by feature 1. Using the same dynamo model as Blanc and Richmond, he calculated the separate predicted contributions of the two dynamos to the observed drifts. The result is displayed in Fig. 6: in the top panel, drifts produced by the solar-wind/magnetospheric dynamo alone are plotted as a function of local time for three different values of the Hall-to-Pedersen height-integrated conductivity ratios. One sees that in all three cases the local time variation of the observationally-derived average disturbance drifts is reasonably well reproduced, but the model predictions fail to adjust to the bulk westward displacement of the observed disturbance drift average values (full curve on the two panels, same as the full curve in the bottom panel of Fig. 2) by about 50 to 100 m/s. When the zonal drifts predicted for the ionospheric disturbance dynamo are added (bottom panel), the fit becomes much better and the westward trend of disturbance drifts is well reproduced. This result showed, not only that the conjugate action of the two dynamos is needed to explain midlatitude storm-time disturbances of electrodynamic parameters, but moreover that their superposed effects indeed well reproduce the total disturbances observed in an average sense.

Further studies developed, quite logically, in two complementary directions. Many efforts were successfully accomplished to extend the set of relevant data, reaching out into a description of their seasonal, solar cycle and activity, and longitude dependences. These works will be described extensively in Sect. 3. In parallel, new types of simulation studies allowing to go beyond the limitations of the Blanc-Richmond model were performed. They included in particular full 3-D descriptions of the thermosphere and its dynamic and ener-

getic response to auroral heating, and a capability for taking into account the different types of variability mentioned above. They will now be briefly described.

Mechanistic Studies Major progress in the study of disturbance-dynamo processes became possible with the applications of fully three-dimensional, time-dependent models of the coupled thermosphere-ionosphere system. Fuller-Rowell et al. (2002) simulated an idealized storm, with an abrupt increase of high-latitude magnetosphere forcing that was then held constant for 12 hours, using the Coupled Thermosphere Ionosphere Plasmasphere Electrodynamic (CTIPE) model. Six hours after the storm onset, changes in the low-latitude electron density were apparent due to changes in vertical plasma drifts similar to those predicted by the simpler modeling of Blanc and Richmond (1980). Fuller-Rowell et al. (2002) found that changes in the equatorial vertical drifts appeared soon after the storm onset, even before the traveling atmospheric disturbances launched by the storm had reached the equator. They pointed out that the storm-time equatorward wind surge at midlatitudes alters the generation of electric fields that are transmitted almost instantaneously to the equator. This phenomenon was further supported by simulations presented by Fuller-Rowell et al. (2008).

Richmond et al. (2003) used the Magnetosphere-Thermosphere-Ionosphere-Electrodynamics General-Circulation Model of Peymirat et al. (1998) to study the effects of complex electrodynamic interactions among the thermosphere, ionosphere, and inner magnetosphere for a simulated magnetic storm. They found the strongest winds and electrodynamic effects on the night side of the Earth, owing in part to a contribution to the night-side winds by strong ion-drag forcing from high-latitude ion convection, with part of the momentum carried to middle latitudes at night by equatorward winds. The modeled electrodynamic effects were similar to those predicted by the simulation of Blanc and Richmond (1980) that used winds existing only on the night side. The electric potential created by the disturbance winds was positive at the equator around midnight, and was associated with equatorial vertical drifts that were downward in the evening and upward in the pre-sunrise hours. Similar results were found by Fuller-Rowell et al. (2008). Richmond et al. (2003) pointed out that changes in the coupled magnetosphere-ionosphere electrodynamics at middle and low-latitudes following a storm are caused not only by the disturbance dynamo, but also by changes in penetration electric fields associated with storm-produced alterations of plasma pressure in the magnetospheric ring current.

Huang et al. (2005) used the Thermosphere-Ionosphere-Electrodynamics General-Circulation Model (TIEGCM) to examine the responses to increased steady-state magnetospheric forcing and to an abrupt termination of the forcing. Similar to Richmond et al. (2003) they found the strongest storm-time disturbance winds on the night side and the associated electric potential maximizing at the equator around midnight. When the magnetospheric forcing was turned off, the midlatitude westward winds became more zonally symmetric within several hours, but they then decayed more slowly over the next few days. The disturbance of the electric potential also became more zonally symmetric, such that the evening and early-morning disturbance vertical plasma drifts at the equator were reduced over a few hours, while the midlatitude westward drifts, day-side downward drifts, and night-side upward drifts decayed much more slowly. In different but related simulations, Huang and Chen (2008) quantified how the equatorial disturbance-dynamo zonal and vertical electric fields develop in time as a simulated storm develops. Their work indicates that during March equinox and June solstice moderate solar flux conditions the disturbance dynamo zonal electric fields are altitude independent at all local times. On the other hand, the evening and late night March equinox vertical electric fields are height independent only above about 400 km. The vertical electric fields shortly after sunset are downward and upward below and above

about 300 km, respectively. These results suggest that disturbance dynamo effects can significantly decrease the shear in the zonal plasma flow below the F layer peak during March equinox. The March equinox late night upward electric fields decrease up to about 300 km and do not change at higher altitude. A further modeling study by Huang (2013) showed longitudinal, seasonal, and solar cycle variations of the disturbance-dynamo effects.

Maruyama et al. (2005, 2007, 2011) coupled CTIPE with the Rice Convection Model (RCM) to examine the complex interactions and feedbacks between the magnetospheric and ionospheric dynamos. They showed how the direct-penetration electric field affects global ionospheric conductivity and winds, especially at night, in a way that interacts with disturbance winds, so that the direct-penetration and disturbance-dynamo electric fields interact with each other. Maruyama et al. (2011) pointed out that preconditioning of both the magnetosphere and the thermosphere/ionosphere by one storm affects the way the coupled system responds to a subsequent storm. The efficiency of shielding between high- and low-latitude electrodynamics is increased by the storm-time increase in both ring-current plasma and the high-speed thermospheric winds generated in the auroral zone. Maruyama and Nakamura (2007) pointed out how storm-time changes of ion drag associated with disturbance-dynamo alterations of plasma drifts can provide a positive feedback for the neutral winds and electric fields, thereby enhancing ionospheric storms.

Pedatella and Forbes (2011) used the TIEGCM to simulate plasma drifts associated with recurrent solar-wind corotating-interaction-region (CIR) disturbances of the magnetosphere and ionosphere, for comparison with zonal and vertical plasma drifts measured around dawn and dusk by the DMSP F13 spacecraft. They performed a superposed-epoch analysis on the model and observation results for the entire year 2005 in terms of key dates of passage of CIRs. Although the modeled drifts were weaker than the observations, which suggested underestimation of Joule heating in the model, most of the modeled features agreed with the observations.

Event Simulations When models are applied to specific time-varying storm events, their predictions become more complicated, and agreement with observations has had mixed success. Mazaudier et al. (1987) used a two-dimensional model to simulate disturbance winds and electric fields for specific storms observed at a midlatitude location, with high-latitude heating proportional to the AE index. Given the simplicity of the model, an encouraging amount of agreement with the observations was achieved. Maruyama et al. (2007) simulated the storms of 2001 March 31 and 2002 April 17–18 with the coupled CTIPE-RCM models. They found surprisingly good overall agreement between the simulations and observations of equatorial vertical drifts during moderately disturbed times. By selectively turning off either the magnetospheric source or the ionospheric dynamo source in separate simulations, they could demonstrate the relative importance of each: while direct-penetration fields tend to dominate in the early hours of a storm, the disturbance dynamo often dominates during later hours. Fuller-Rowell et al. (2008) showed how the simulated vertical drifts at the equator for the storm of 2004 November 7–10 change from one day to the next during the storm. Zaka et al. (2010) found that a TIEGCM storm simulation for 1993 June 21 underestimated the observed disturbance of equatorial geomagnetic variations, and suggested that the storm-time energy inputs were underestimated in the model. Klimenko and Klimenko (2012) simulated the 2006 December 15–17 magnetic storm with the Global Self-consistent Model of the Thermosphere, Ionosphere, Protonosphere (GSM TIP) (Namgaladze et al. 1998) in the American sector, conducting simulations with and without ionospheric dynamo effects in order to quantify the influence of the quiet and disturbance dynamos. This study suggests that the disturbance dynamo mechanism leads to increased daytime equatorial eastward electric

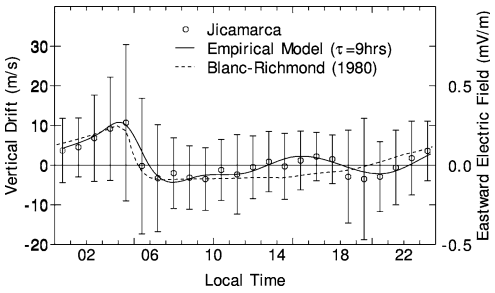

Fig. 7 Comparison of the empirical equatorial disturbance dynamo vertical drift pattern and of the Blanc-Richmond model result for an increase in the hemispheric power input corresponding to 400 nT. The data points with the standard deviations (not error) bars were obtained by binning the residual drifts for model conditions (after Scherliess and Fejer 1997)

fields and to stronger Equatorial Ionospheric Anomaly (EIA), which is not consistent results from other studies and with the predictions from the Blanc-Richmond model.

3 Experimental Results

Low-latitude disturbance dynamo electric fields have been extensively studied using equatorial F-region plasma drift and electrojet magnetic field measurements (e.g., Fejer et al. 1983; Sastri 1998; Mazaudier and Venkateswaran 1990; Fejer and Scherliess 1995, 1997; Scherliess and Fejer 1997; Zaka et al. 2009; Fathy et al. 2014; Yamazaki and Kosch 2015; Xiong et al. 2016). Midlatitude disturbance dynamo studies have largely relied on zonal plasma drift observations (e.g., Blanc 1983a, 1983b; Fejer and Emmert 2003; Scherliess and Fejer 1998; Kumar et al. 2010), although Pedatella and Forbes (2011) also examined vertical drifts.

Average Morphology Scherliess and Fejer (1997) used F-region vertical drifts measured by the Jicamarca radar and auroral electrojet indices to study and model empirically the temporal evolution of equatorial perturbation drifts driven by disturbance dynamo zonal electric fields. They showed that these perturbation drifts last for up to about 30 hours after large energy depositions into the high-latitude ionosphere during periods of enhanced geomagnetic activity. Scherliess and Fejer (1997) pointed out that, on the average, the equatorial disturbance zonal electric fields can be described by two major components with time delays of about 1–12 hours and 22–28 hours after high-latitude current enhancements. The shortest delay disturbance drifts result from the dynamo effects of storm-driven fast traveling atmospheric disturbances (e.g., Fuller-Rowell et al. 2002). Shortly after geomagnetic quieting, they are also driven by fossil winds equatorward of the shielding layer, and by overshielding prompt penetration electric fields (e.g., Spiro et al. 1988; Richmond et al. 2003). The disturbance dynamo drifts with the longest time delays are associated with storm-driven changes in the thermosphere circulation and with ionospheric composition changes (e.g., Fuller-Rowell et al. 2002).

Figure 7 shows the generally excellent agreement between the disturbance dynamo drifts from the Blanc-Richmond theoretical model and the empirical drifts after nine hours of high-latitude energy deposition. In this case, the simulated drifts were scaled down to match the value corresponding to 400 nT used in the empirical model. The large scatter bars in the binned data, which are much larger than the measurements error bars and the standard errors of the means, are mostly due to the large quiet-time variability of the equatorial quiet-time drifts. Figure 7 shows that the disturbance drifts are small and generally downward during the day and upward with larger values at night, particularly in the postmidnight period. The Scherliess-Fejer empirical model indicates that for time delays of about

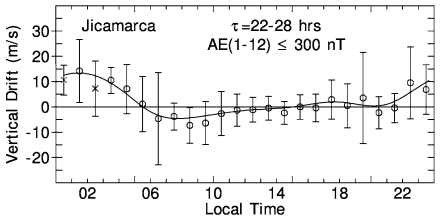

Fig. 8 Long-term disturbance dynamo empirical model drifts after a geomagnetic quiet period preceded by a disturbed 22–28 h period with an increase in the AE indices by 400 nT. The data points with the standard deviation (not error) bars were obtained by binning the residual drifts for model conditions (after Scherliess and Fejer 1997)

13–20 hours the equatorial vertical disturbance drifts are essentially independent of storm time enhancements in the high-latitude current system. Large nighttime vertical disturbance drifts were also shown to occur with time delays of about 20–30 hours when geomagnetic storm activity is followed by several hours of quiet conditions. Figure 8 illustrates the local time dependence of disturbance dynamo drifts during short-term (1–12 h) magnetic quiet conditions preceeded by long-term moderate or strong storm conditions (i.e., average $AE(22–28\ \text{h}) > 350$ nT). These perturbation drifts again have largest values at night with peak amplitudes at about 0100 LT.

The equatorial disturbance dynamo drifts exhibit large seasonal, solar cycle, and longitudinal dependences which we are going to describe now.

Seasonal and Solar Flux Variations Jicamarca radar measurements show that disturbance dynamo effects lead to larger decreases in the evening upward drifts at equinox than during June solstice, and to nearly identical postmidnight disturbance drift effects during these seasons (Fejer 2002). Equatorial longitudinally averaged ROCSAT-1 satellite ion drift measurements at an altitude of about 600 km showed largest equatorial vertical evening downward disturbance dynamo drifts during equinox and smallest ones during June solstice, while the nighttime upward perturbation drifts were largest during December solstice and nearly identical during equinox and June solstice (Fejer et al. 2008). These results are illustrated in Fig. 9. The occurrence of smaller disturbance dynamo downward drifts near dusk during June solstice than during equinox is in good agreement with the TIEGCM simulations presented by Huang and Chen (2008). The daytime perturbation drifts derived from ROCSAT-1 were small and highly variable, and did not provide reliable information on possible seasonal dependence. ROCSAT-1 and Jicamarca measurements suggest that the equatorial disturbance dynamo vertical drifts increase with solar flux near dusk, and that the nighttime drifts do not change much with solar flux. Studies of post sunset F layer height changes in the Indian equatorial region indicated that, except for the early night period, the duration of short and long term disturbance dynamo effects decreases with increasing solar flux (Kakad et al. 2011). The delays for largest vertical drift perturbations were found to be 0.5–4 hours and 16–23 hours for short and long term effects, respectively.

Longitudinal Variations Figure 10 shows the longitudinal dependence of equatorial vertical disturbance dynamo drifts during equinox obtained by averaging the ROCSAT-1 residual drifts in 120° wide, 60° overlapping bins. The evening downward and the nighttime upward perturbation drifts are largest in the eastern and western hemisphere, respectively. The largest downward and upward drifts occur about 180° apart, which is consistent with curl-free disturbance drifts. As mentioned earlier, the small daytime derived perturbation

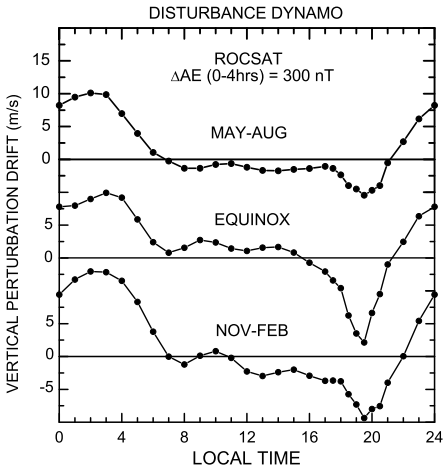

Fig. 9 Longitudinally averaged F-region equatorial disturbance dynamo vertical plasma drifts derived from ROCSAT-1 satellite data (after Fejer et al. 2008)

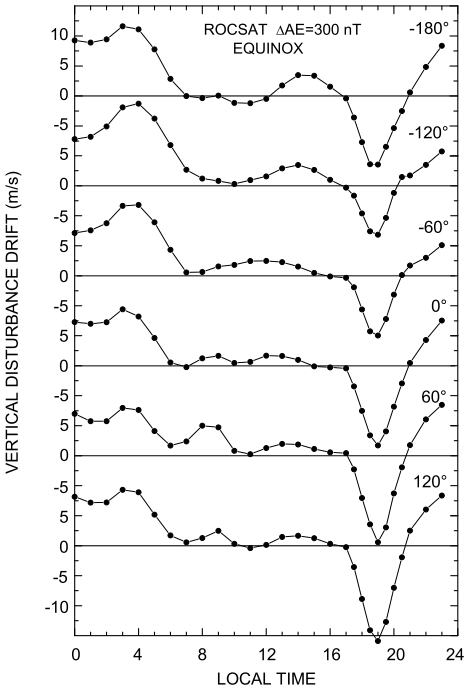

Fig. 10 Longitudinal variation of equatorial F-region vertical disturbance dynamo plasma drifts during equinox (after Fejer et al. 2008)

drifts have no statistical significance. Figure 11 presents a comparison of equinoctial disturbance dynamo vertical drifts at 60°E and 75°W derived from TIEGCM simulations of Huang et al. (2005). These perturbation drifts are larger in the postmidnight sector near dawn at 75°W than at 60°E while the opposite is the case near dusk, in good agreement with the data shown in Fig. 10. Huang (2013) showed that the longitude variations of disturbance-dynamo electric fields also depend on season and solar activity. As discussed below, Yamazaki and Kosch (2015) and Xiong et al. (2016) found significant longitude differences in day-time disturbances of the equatorial electrojet during storm recovery.

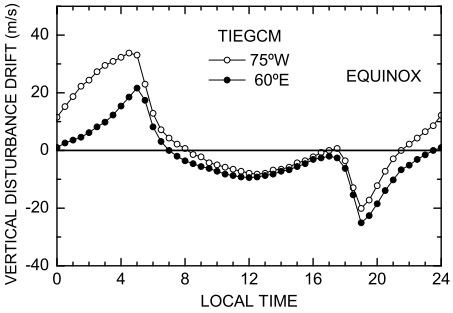

Fig. 11 Equatorial vertical disturbance dynamo vertical drifts during equinox at two longitudes obtained by Huang et al. (2005) from TIEGCM simulations (after Fejer et al. 2008)

Latitudinal Variations Several studies have examined the latitudinal profiles of the magnetic signatures of daytime disturbance dynamo zonal electric fields (e.g., Fambitakoye et al. 1990; LeHuy and Amory-Mazaudier 2005; Zaka et al. 2009, 2010; Fathy et al. 2014). In equatorial studies, magnetospheric current effects are generally removed by subtracting off-equatorial from equatorial horizontal magnetic field measurements. They showed that the low-latitude daytime disturbance dynamo currents are westward, as a result of westward perturbation electric fields, which is consistent with the predictions of the Blanc-Richmond theory and with radar plasma drift measurements (e.g., Zaka et al. 2009; Fathy et al. 2014). These current perturbations are significantly enhanced near the magnetic equator due to a large daytime Cowling conductivity at electrojet heights. The mid-latitude disturbance dynamo currents are eastward, which is opposite to the quiet time ionospheric currents. Zaka et al. (2010) showed that TIEGCM disturbance dynamo simulations reproduced the anti-quiet middle and low-latitude current system driven by disturbance dynamo electric fields during 21 June 1993, but significantly underestimated their amplitudes. Fathy et al. (2014) reported the occurrence on several days of disturbance dynamo perturbations of middle and low-latitude ionospheric currents in the European-African, Asian, and American sectors during a period of high-speed solar wind streams associated with a coronal hole on 5–10 April 2010, which was preceded by a large coronal mass ejection. They reported strongest disturbance dynamo effects in the European-African sector with reductions in the amplitude of the low-latitude daytime H component, in agreement with the Blanc-Richmond model.

Equatorial Electrojet Effects Yamazaki and Kosch (2015) presented a detailed study of substorm and storm-driven equatorial electrojet perturbations using very extensive ground-based magnetometer measurements in the Peruvian and Indian sectors. As is usually the case, magnetospheric current effects were removed by subtracting horizontal magnetic field measurements at equatorial and off-equatorial sites in the same longitudinal sector. Figure 12 shows the daytime equatorial electrojet current perturbations over Peru and India during 7–12 hours into storm recovery, as defined by the minima of the Dst index. The Indian data shows a westward current disturbance with a maximum near noon. On the other hand, the Peruvian electrojet data is characterized by a semidiurnal variation with a current disturbance which is westward in the morning and eastward in the afternoon, in very good agreement with the empirical disturbance dynamo vertical drift pattern shown in Fig. 7. Yamazaki and Kosch (2015) also reported the increase of the electrojet current disturbances from solar minimum to maximum, probably as a result of enhanced ionospheric conductivities. In addition, a significant seasonal dependence was observed in the Indian sector, with the largest disturbances during December solstice months and the smallest ones during June solstice months, but no seasonal dependence was evident in the Peruvian electrojet data.

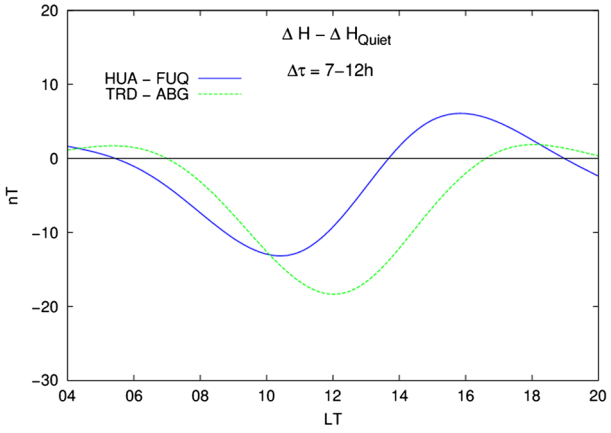

Fig. 12 Equatorial electrojet daytime horizontal magnetic field perturbations over India and Peru 7–12 hours into storm recovery phases and for moderate solar flux conditions (after Yamazaki and Kosch 2015)

Disturbance dynamo electrojet perturbations following storms and substorms have similar local time dependence, but the latter are shorter-lived (Yamazaki and Kosch 2015). Xiong et al. (2016) showed the longitudinal variation of equatorial electrojet afternoon disturbance drift patterns derived from CHAMP satellite measurements is consistent with the results presented by Yamazaki and Kosch (2015). This latter study also indicated that the response of the ionosphere to disturbance dynamo effects is faster in the F- than in the E-region.

Zonal Drift Effects Middle and low-latitude meridional (vertical at the equator) disturbance dynamo electric fields, which drive F-region zonal drift perturbations, have not been examined in as much detail as the zonal electric fields. The characteristics of these disturbance dynamo electric fields have often been inferred from the study of average zonal perturbation drifts obtained by subtracting quiet-time from storm-time values. We already presented in Sect. 1 the incoherent scatter radar measurements of F-region zonal disturbance drifts over Saint-Santin by Blanc (1983a) and in Sect. 2 their interpretation as resulting from the combined effects of the solar-wind/magnetosphere and ionospheric disturbance dynamos (Blanc 1983b). Short-lived prompt penetration drifts tend to cancel out, but this is not the case for perturbation drifts driven by steady-state leakage of high altitude electric fields during disturbed periods of weak shielding, and by overshielding electric fields following geomagnetic quieting. Scherliess et al. (2001) showed that over Millstone Hill (42.6°N, 288.5°E, apex magnetic latitude 54°) the zonal disturbance drifts have significant amplitudes at night even for $Kp < 3$ (6-hour average of 1.8), with largest values near midnight. This is not the case for perpendicular northward disturbance drifts.

Low- and middle-latitude F-region average zonal disturbance drifts determined from Dynamics Explorer-2 (DE-2) satellite ion drift meter measurements (Coley and Heelis 1989; Heelis and Coley 1992) during periods of enhanced geomagnetic activity were in good agreement with the Saint-Santin data, as are night-time disturbance drifts from the Hokkaido radar (Zou and Nishitani 2014). Burch et al. (2004) noted that the subrotation of the plasmasphere with respect to the Earth during disturbed periods, corresponding to westward plasma drifts at ionospheric upper-midlatitudes, is consistent with disturbance-dynamo theory.

Scherliess and Fejer (1998) used DE-2 satellite measurements and auroral AE indices to study and model empirically the longitudinal and temporal dependence of F-region low- and mid-latitude (invariant latitudes $20° < \Lambda < 60°$) prompt penetration and disturbance dynamo zonal drifts. In this case, measurements taken poleward of the predicted maximum expansion of the auroral zone were excluded and the effects of auroral drifts were minimized

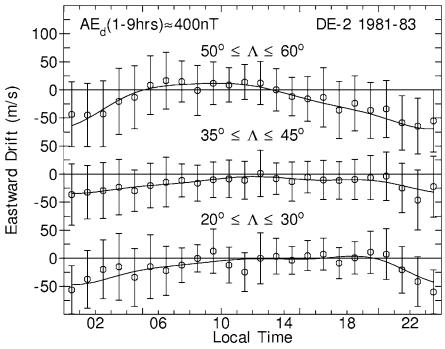

Fig. 13 Long-lasting zonal plasma drift perturbations in three invariant latitudinal ranges for an average increase in geomagnetic activity by 400 nT over a period of 9 hours. The *scatter bars* denote the standard deviations, and the *solid curves* indicate empirical model results (after Scherliess and Fejer 1998)

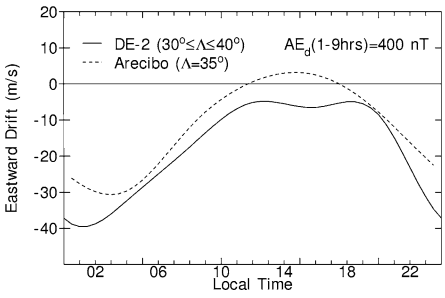

Fig. 14 DE-2 and Arecibo disturbance dynamo model drifts following 9 hours of enhanced geomagnetic activity (after Scherliess and Fejer 1998)

by limiting the perturbation drifts to values under 150 m/s. Figure 13 presents the local time dependence of the perturbation drifts corresponding to an average 400 nT increase in the AE indices over the quiet time (130 nT) value during the previous 9 hours. Figure 13 shows small eastward or near-zero daytime drifts shifting to earlier local times with increasing latitude and larger westward nighttime drifts with peak values close to midnight. These perturbation drifts are generally in good agreement with results derived from Saint-Santin (Blanc 1983b), Arecibo (Fejer 1997) and Millstone Hill (Scherliess et al. 2001) radars, and earlier DE-2 results presented by Heelis and Coley (1992). Scherliess et al. (2001) showed that the short-term meridional disturbance drifts over Millstone Hill [42.6°N, 288.5°E, magnetic latitude 54°] decay faster than the zonal disturbance drifts, which is consistent with the faster decay of the meridional disturbance winds (e.g., Huang et al. 2005). These results are also consistent with disturbance drifts derived from digisonde measurements from Bundoora (145.1°E, 37.7°S, 49°S magnetic), which were interpreted as due to disturbance dynamo electric fields (Kumar et al. 2010). This latter study also showed that in the dusk to midnight local time sector these disturbance drifts last up to about 50 hours. Zou and Nishitani (2014) reported disturbance dynamo effects between 44° and 53° geomagnetic latitude lasting from 5 to 20 h, with maximum values at 12 h, after substorm onset.

Figure 14 shows a comparison of the Arecibo (18°N, 67°W, 35° invariant latitude) and DE-2 disturbance dynamo model drifts. These results were derived using the procedure described by Fejer and Scherliess (1995) to account for prompt penetration electric field effects. However, as pointed out by Blanc (1983b), it is experimentally very difficult to fully decouple perturbation drifts due to various sources of disturbance electric fields, especially the steady-state leakage of high-latitude electric fields.

Fejer et al. (2005) developed empirical models of quiet-time and disturbed equatorial F-region zonal plasma drifts using Jicamarca incoherent scatter radar measurements between 1970 and 2003. These models show larger amplitude nighttime westward perturbation drifts

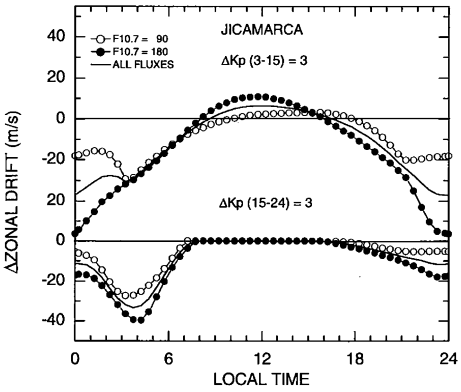

Fig. 15 Jicamarca F-region model disturbance drifts corresponding to $\Delta Kp = 3$ over 2 preceding periods. The *solid curves* denote the model drifts for moderate solar flux conditions (after Fejer et al. 2005)

during equinox and December solstice than during June solstice, which were attributed to disturbance dynamo electric field effects. As mentioned earlier, the equatorial F-region vertical disturbance drifts near dusk have similar seasonal dependence. Figure 15 shows the equinoctial and December solstice Jicamarca empirical zonal disturbance drifts after 3–15 and 15–24 hours of enhanced geomagnetic activity. These disturbance drifts are eastward with small values during the day and westward with much larger magnitude values at night, and increase with solar flux. Near dusk the perturbation drifts are westward and increase with local time. As mentioned earlier, the TIEGCM simulations presented by C.M. Huang and Chen indicate that the disturbance dynamo zonal drifts in the early evening are eastward at the lowest altitudes and westward at higher altitudes. It is important to note, that the Jicamarca F-region drifts correspond to height averages typically between about 250 and 800 km, and that over this height range the zonal drifts exhibit large altitudinal variations near dusk and in the early night sector, which is not the case for the vertical drifts. The peak westward drifts occur at about 04 LT, in good agreement with the Blanc-Richmond and C.M. Huang and Chen model drifts, except in the short-term high solar flux case, when they peak around midnight. The June solstice zonal perturbation drifts are much smaller and are largely confined to the midnight sector (Fejer et al. 2005).

DMSP17 satellite measurements during the January–April 2007 period of high solar wind streams showed that, as the solar wind speed changed from 300 to 700 km with increasing magnetic activity, the equatorial zonal and vertical plasma drifts at about 1730 LT at 840 km altitude varied from -40 to 40 m/s and 10 to -10 m/s, respectively (Huang 2012). These eastward and downward perturbations were consistent with disturbance dynamo electric field effects.

4 Summary and Conclusions

We have found that the Blanc-Richmond disturbance dynamo theory can account for the main characteristics of storm and post-storm middle and low-latitude ionospheric currents and electric field disturbances due to enhanced energy deposition into the high-latitude ionosphere. Studies using three-dimensional models of thermosphere/ionosphere dynamics and electrodynamics have further elaborated the theory by describing more realistically the temporal evolution, spatial and seasonal variations, and solar-activity dependence of disturbance-dynamo effects for particular high-latitude energy inputs, and have shown

how the disturbance dynamo interacts with direct-penetration electric fields. Recent studies indicate that TIEGCM simulations underestimate disturbance dynamo magnetic field and plasma drift amplitudes when the high-latitude energy input is not symmetric between the hemispheres (Zaka et al. 2010; Huang 2013). These simulations have not examined the characteristics of longer lasting (over 12 h) disturbance dynamo effects, which appear to be particularly important at low-latitudes. Additional studies are needed to further improve the understanding of the temporal and spatial variability of disturbance-dynamo effects for different types of storm energy inputs.

The season dependent longitudinal variation of mid-latitude disturbance dynamo electric fields and currents still remains to be determined. In this region, prompt penetration and steady state leakage of high-latitude electric fields makes the identification of disturbance dynamo electric fields difficult even during relatively low levels of geomagnetic activity, and IMF By effects cause large changes in the perturbation electric fields (e.g., Foster et al. 1986). This is particularly the case for the zonal disturbance drifts. On the other hand, since the zonal disturbance drifts are larger and longer lasting than the meridional drifts, they can be more readily studied during post-storm periods.

Disturbance dynamo electric fields, drifts and currents have been studied most extensively at low-latitudes where high-latitude prompt penetration and leakage electric field effects can be accounted for more easily. In this region, the initial model results on their seasonal and longitudinal effects on the equatorial electrojet and zonal electric fields are generally in good agreement with observations, but they still need to be determined in more detail in response to various high-latitude heating sources and storm conditions. The solar cycle dependence of short- and long-term equatorial nighttime disturbance zonal dynamo electric fields suggested by Kakad et al. (2011) need to be examined in other longitudinal sectors. This is particularly the case in the American sector, where very large longitudinal effects have been inferred from GPS TEC measurements during and after disturbed periods (e.g., Liu et al. 2014; Fagundes et al. 2016). The altitudinal dependence of the vertical and zonal disturbance dynamo plasma drifts in the equatorial lower ionosphere also need to be studied in more detail since they can play important roles in the generation of plasma irregularities. The seasonal, longitudinal and altitudinal variations and lifetimes of the equatorial zonal disturbance drifts is not well understood, especially during December solstice.

The study of the extensive electrodynamic ground-based observations, measurements from the CHAMP, C/NOFS, DMSP, Swarm and from the upcoming ICON satellites and complementary numerical simulations using general circulation models could provide a deeper understanding of the temporal and spatial variations of disturbance dynamo electrodynamic disturbances. More extensive numerical simulations of both meridional and zonal disturbance dynamo electric fields (which generally have not been done in recent studies) are particularly needed to guide the experimental studies. These complementary future studies would significantly improve the understanding and forecasting of post-storm ionospheric plasma density variations, TEC, and the occurrence of low-latitude ionospheric plasma structure and irregularities and scintillations which can affect communication and navigation systems.

Acknowledgements The work at Utah State University was supported by the Aeronomy Program, Division of Atmospheric Sciences of the National Science Foundation through grant AGS-1068104. ADR was supported in part by NASA grants NNX13AD64G and NNX14AE08G. The National Center for Atmospheric Research is sponsored by the National Science Foundation.

References

M.A. Abdu, T. Maruyama, I.S. Batista, S. Saito, M. Nakamura, Ionospheric response to the October 2003 superstorm: longitudinal/local time effects over equatorial low and middle latitudes. J. Geophys. Res. **112**, A10306 (2007). doi:10.1029/2006JA012228

M. Blanc, Mid-latitude convection electric fields and their relation to ring current development. Geophys. Res. Lett. **5**, 203–206 (1978)

M. Blanc, Magnetospheric convection effects at mid-latitudes 1. Saint-Santin observations. J. Geophys. Res. **88**, 211–213 (1983a)

M. Blanc, Magnetospheric convection effects at mid-latitudes 3. Theoretical derivation of the disturbance convection pattern in the plasmasphere. J. Geophys. Res. **88**, 235–251 (1983b)

M. Blanc, A.D. Richmond, The ionospheric disturbance dynamo. J. Geophys. Res. **85**(A4), 1669–1686 (1980). doi:10.1029/JA085iA04p01669

J.L. Burch, J. Goldstein, B.R. Sandel, Cause of plasmasphere corotation lag. Geophys. Res. Lett. **31**, L05802 (2004). doi:10.1029/2003GL019164

R.W. Coley, R.A. Heelis, Low latitude zonal and vertical ion drifts seen by DE-2. J. Geophys. Res. **94**, 6751–6761 (1989)

P.R. Fagundes, F.A. Cardoso, B.G. Fejer, K. Venkatesh, B.A.G. Ribeiro, V.G. Pillat, GPS-TEC ionospheric storm effects during the extreme space weather event of March 2015 over the Brazilian sector. J. Geophys. Res. Space Weather **121** (2016). doi:10.1002/2015JA022214

O. Fambitakoye, M. Menvielle, C. Mazaudier, Global disturbance of the transient magnetic field associated with thermospheric storm winds on March 23, 1979. J. Geophys. Res. **95**, 15209–15218 (1990). doi:10.1029/JA095iA09p15209

I. Fathy, C. Amory-Mazaudier, A. Fathy, A.M. Mahrous, K. Yumoto, E. Ghamry, Ionospheric disturbance dynamo associated to a coronal hole: case study of 5–10 April 2010. J. Geophys. Res. Space Phys. **119**, 4120–4133 (2014). doi:10.1002/2013JA019510

B.G. Fejer, The electrodynamics of the low latitude ionosphere: recent results and future challenges. J. Atmos. Sol.-Terr. Phys. **59**, 1456–1482 (1997). doi:10.1016/s1364-6826(96)00149-6

B.G. Fejer, Low latitude storm time ionospheric electrodynamics. J. Atmos. Sol.-Terr. Phys. **64**, 1401–1408 (2002)

B.G. Fejer, Low latitude ionospheric electrodynamics. Space Sci. Rev. **158**(1), 145–166 (2011). doi:10.1007/s11214-010-9690-7

B.G. Fejer, L. Scherliess, Time dependent response of equatorial ionospheric electric fields to magnetospheric disturbances. Geophys. Res. Lett. **22**, 851–854 (1995). doi:10.1029/95GL00390

B.G. Fejer, L. Scherliess, Empirical models of storm time equatorial zonal plasma drifts. J. Geophys. Res. **102**(A11), 24047–24056 (1997). doi:10.1029/97JA02164

B.G. Fejer, J.T. Emmert, Low-latitude ionospheric disturbance electric field effects during the recovery phase of the 19–21 October 1998 magnetic storm. J. Geophys. Res. **182**(A12), 1454 (2003). doi:10.1029/2003JA010190

B.G. Fejer, M.F. Larsen, D.T. Farley, Equatorial disturbance dynamo electric fields. Geophys. Res. Lett. **10**, 537–540 (1983)

B.G. Fejer, R.W. Spiro, R.A. Wolf, J.C. Foster, Latitudinal variation of perturbation electric fields during magnetically disturbed periods: 1986 SUNDIAL observations and model results. Ann. Geophys. **8**(6), 441–454 (1990)

B.G. Fejer, E.R. de Paula, S.A. Gonzalez, R.F. Woodman, Average vertical and zonal *F* region plasma drifts over Jicamarca. J. Geophys. Res. **96**(A8), 13901–13906 (1991). doi:10.1029/91A01171

B.G. Fejer, J.R. Souza, A.S. Santos, A.E.C. Perreira, Climatology of *F* region zonal drifts over Jicamarca. J. Geophys. Res. **110**, A12310 (2005). doi:10.1029/2005JA011324

B.G. Fejer, J.W. Jensen, T. Kikuchi, M.A. Abdu, J.L. Chau, Equatorial ionospheric electric fields during the November 2004 magnetic storm. J. Geophys. Res. **112**, A10 (2007). doi:10.1029/2007JA012376

B.G. Fejer, J.W. Jensen, S.-Y. Su, Seasonal and longitudinal dependence of equatorial disturbance vertical plasma drifts. Geophys. Res. Lett. **35**, L20106 (2008). doi:10.1029/GL2008035584

J.C. Foster, J.M. Holt, R.G. Musgrove, D.S. Evans, Solar wind dependencies of high-latitude convection and precipitation, in *Solar Wind Magnetosphere Coupling*, ed. by Y. Kamide, J.A. Slavin (Terra Sci., Tokyo, 1986), pp. 477–494

J.C. Foster, P.J. Erickson, A.J. Coster, J. Goldstein, F.J. Rich, Ionospheric signature of plasmaspheric tails. Geophys. Res. Lett. **29**(13), 1623–1626 (2002). doi:10.1029/GL015067

T.J. Fuller-Rowell, G.H. Millward, A.D. Richmond, M.V. Codrescu, Storm-time changes in the upper atmosphere at low latitudes. J. Atmos. Sol.-Terr. Phys. **64**, 1383–1391 (2002)

T.J. Fuller-Rowell, A.D. Richmond, N. Maruyama, Global modeling of storm-time thermospheric dynamics and electrodynamics, in *Midlatitude Ionospheric Dynamics and Disturbances*, ed. by P.M. Kintner Jr., A.J. Coster, T. Fuller-Rowell, A.J. Mannucci, M. Mendillo, R. Heelis. Am. Geophys. Union Geophysical Monograph, vol. 181 (2008), pp. 187–200

C.A. Gonzales, M.C. Kelley, B.G. Fejer, J.F. Vickrey, R.F. Woodman, Equatorial electric fields during geomagnetically disturbed conditions: implications of simultaneous auroral and equatorial measurements. J. Geophys. Res. **84**, 5803–5812 (1979)

R.A. Heelis, W.R. Coley, East-West ion drifts at mid-latitudes observed by dynamics explorer-2. J. Geophys. Res. **97**, 19461–19469 (1992)

C.M. Huang, Disturbance dynamo electric fields in response to geomagnetic storms occurring at different universal times. J. Geophys. Res. Space Phys. **118**, 496–501 (2013). doi:10.1029/2012JA018118

C.M. Huang, M.Q. Chen, Formation of maximum electric potential at the geomagnetic equator by the disturbance dynamo. J. Geophys. Res. **113**, A03301 (2008). doi:10.1029/2007JA012843

C.M. Huang, A.D. Richmond, M.-Q. Chen, Theoretical effects of geomagnetic activity on low latitude electric fields. J. Geophys. Res. **110**, A5 (2005). doi:10.1029/2004JA010994

C.S. Huang, Equatorial ionospheric electrodynamics associated with high-speed solar wind streams during January–April 2007. J. Geophys. Res. **117**, A10311 (2012). doi:10.1029/2012JA017930

C.S. Huang, Storm-to-storm main phase repeatability of the local time variation of disturbed low-latitude vertical ion drifts. Geophys. Res. Lett. **42**, 5694–5701 (2015). doi:10.1002/2015GL064674

C.S. Huang, S. Sazykin, J.L. Chau, N. Maruyama, M.C. Kelley, Penetration of electric fields: efficiency and characteristic time scale. J. Atmos. Sol.-Terr. Phys. **69** (2007). doi:10.1016/j/jastp.2006.08.06

C.S. Huang, F.J. Rich, W.J. Burke, Storm-time electric fields in the equatorial ionosphere observed near the dusk meridian. J. Geophys. Res. **115**, A08313 (2010). doi:10.1029/2009JA015150

B. Kakad, D. Tiwari, T.K. Pant, Study of disturbance dynamo effects at nighttime equatorial F region in Indian longitude. J. Geophys. Res. **116**, A12318 (2011). doi:10.1929/2011JA016626

M.C. Kelley, *The Earth's Ionosphere: Plasma Physics and Electrodynamics* (Academic Press, San Diego, 1988)

M.C. Kelley, B.G. Fejer, C.A. Gonzales, An explanation for anomalous equatorial ionospheric electric fields associated with a northward turning of the interplanetary magnetic field. Geophys. Res. Lett. **6**, 301–306 (1979). doi:10.10129/GL006i004p00301

T. Kikuchi, K. Hashimoto, K. Nozaki, Penetration electric fields to the equator during a geomagnetic storm. J. Geophys. Res. **113**, A06214 (2008). doi:10.1029/2007JA012628

M.V. Klimenko, V.V. Klimenko, Disturbance dynamo, prompt penetration electric field and overshielding in the Earth's ionosphere during geomagnetic storm. J. Atmos. Sol.-Terr. Phys. **90–91**, 146–155 (2012). doi:10.1016/j.jastp.2012.02.018

V.V. Kumar, M.L. Parkinson, P.L. Dyson, On the temporal evolution of midlatitude F region disturbance drifts. J. Geophys. Res. **115**, A08325 (2010). doi:10.1029/2009015229

M. LeHuy, C. Amory-Mazaudier, Magnetic signature of the ionospheric disturbance dynamo at equatorial latitudes: Ddyn. J. Geophys. Res. **110**, A02312 (2005). doi:10.1029/2004JA01078

J. Liu, L. Liu, T. Nakamura, B. Zhao, B. Ning, A. Yoshiwaka, A case of ionospheric storm effects during long-lasting southward IMF Bz-driven geomagnetic storm. J. Geophys. Res. **119**, 7716–7731 (2014). doi:10.1002/2014JA020273

N. Maruyama, A.D. Richmond, T.J. Fuller-Rowell, M.V. Codrescu, S. Sazykin, F.R. Toffoletto, R.W. Spiro, G.H. Millward, Interaction between direct penetration and disturbance dynamo electric fields in the storm-time equatorial ionosphere. Geophys. Res. Lett. **32** (2005). doi:10.1029/2005GL023763

N. Maruyama, S. Sazykin, R.W. Spiro, D. Anderson, A. Anghel, R.A. Wolf, F.R. Toffoletto, T.J. Fuller-Rowell, M.V. Codrescu, A.D. Richmond, G.H. Millward, Modeling storm-time electrodynamics of the low-latitude ionosphere-thermosphere system: can long lasting disturbance electric fields be accounted for? J. Atmos. Sol.-Terr. Phys. **69** (2007). doi:10.1016/j.jastp.2006.08.020

N. Maruyama, T.J. Fuller-Rowell, M.V. Codrescu, D. Anderson, A.D. Richmond, A. Maute, S. Sazykin, F.R. Toffoletto, R.W. Spiro, R.A. Wolf, G.H. Millward, Modeling the storm time electrodynamics, in *Aeronomy of the Earth's Atmosphere and Ionosphere*, ed. by M.A. Abdu, D. Pancheva, A. Bhattacharyya (Springer, Dordrecht, 2011), pp. 455–464

T. Maruyama, M. Nakamura, Conditions for intense ionospheric storms expanding to lower midlatitudes. J. Geophys. Res. **112**, A05310 (2007). doi:10.1029/2006JA012226

S. Matsushita, Ionospheric variations associated with geomagnetic disturbances. J. Geomagn. Geoelectr. **5**, 109–135 (1953)

C.A. Mazaudier, A.D. Richmond, D. Brinkman, On thermospheric winds produced by auroral heating during magnetic storms and associated dynamo electric fields. Ann. Geophys. **5A**, 443–448 (1987)

C.A. Mazaudier, S.V. Venkateswaran, Delayed ionospheric effects of the geomagnetic storm of March 22, 1979 studied by the sixth coordinated data analysis workshop (CDAW–6). Ann. Geophys. **8**, 511–518 (1990)

A.A. Namgaladze, Yu.U. Kore'kov, V.V. Klimenko, I.V. Karpov, V.A. Sorokin, V.A. Naumova, Numerical modeling of the thermosphere-ionosphere-protonosphere. J. Atmos. Terr. Phys. **53**(11/12), 113–1124 (1998)
A. Nishida, N. Iwasaki, T. Nagata, The origin of fluctuations in the equatorial electrojet: a new type of geomagnetic variation. Ann. Geophys. **22**, 5549–5559 (1966)
N.M. Pedatella, J.M. Forbes, Electrodynamic response of the ionosphere to high-speed solar wind streams. J. Geophys. Res. **116**, A12310 (2011). doi:10.1029/2011JA017050
C. Peymirat, A.D. Richmond, B.A. Emery, R.G. Roble, A magnetosphere-thermosphere-ionosphere-electrodynamics general-circulation model. J. Geophys. Res. **103**, 17467–17477 (1998)
C. Peymirat, A.D. Richmond, A.T. Kobea, Electrodynamic coupling of high and low latitudes: simulations of shielding/overshielding effects. J. Geophys. Res. **105**, 22991 (2000). doi:10.1029/2000JA000057
C. Peymirat, A.D. Richmond, R.G. Roble, Neutral wind influence on the electrodynamic coupling between the ionosphere and magnetosphere. J. Geophys. Res. **107**, A1 (2002). doi:10.1029/2001JA900106
R.G. Rastogi, The effect of geomagnetic activity on the F2 region over central Africa. J. Geophys. Res. **67**, 1367–1374 (1962)
A.D. Richmond, Ionospheric electrodynamics, in *Handbook of Atmospheric Electrodynamics*, vol. 2, ed. by H. Volland (CRC Press, Boca Raton, 1995), pp. 249–290
A.D. Richmond, S. Matsushita, Thermospheric response to a magnetic substorm. J. Geophys. Res. **80**, 2839–2850 (1975)
A.D. Richmond, C. Peymirat, R.G. Roble, Long-lasting disturbances in the equatorial ionospheric electric field simulated with a coupled magnetosphere-ionosphere-thermosphere model. J. Geophys. Res. **118**(A3), 1118 (2003). doi:10.1029/2002JA009758
J.H. Sastri, Equatorial electric fields of ionospheric disturbance dynamo origin. Ann. Geophys. **6**, 635–642 (1998)
L. Scherliess, B.G. Fejer, Storm-time dependence of equatorial disturbance dynamo zonal electric fields. J. Geophys. Res. **102**, 24037–24046 (1997). doi:10.1029/97JA02165
L. Scherliess, B.G. Fejer, Satellite studies of mid- and low-latitude ionospheric disturbance zonal plasma drifts. Geophys. Res. Lett. **25**, 1503–1506 (1998)
L. Scherliess, B.G. Fejer, J. Holt, L. Goncharenko, C. Amory-Mazaudier, M.J. Buonsanto, Radar studies of midlatitude ionospheric plasma drifts. J. Geophys. Res. **106**(A2), 1771–1783 (2001)
C. Senior, M. Blanc, On the control of magnetospheric convection by the spatial distribution of ionospheric conductivities. J. Geophys. Res. **89**(A1), 261–284 (1984)
R.W. Spiro, R.A. Wolf, B.G. Fejer, Penetration of high-latitude electric field effects to low latitude during SUNDIAL 1984. Ann. Geophys. **6**, 39–50 (1988)
J. Testud, P. Amayenc, M. Blanc, Middle and low latitude effects of auroral disturbances from incoherent-scatter. J. Atmos. Terr. Phys. **37**, 989–1009 (1975)
B. Veenadhari, S. Alex, T. Kikuchi, A. Shinbori, R. Singh, E. Chandrasekar, Penetration of magnetospheric electric fields to the equator and their effects on low latitude ionosphere during intense geomagnetic storms. J. Geophys. Res. **115**, A3 (2010). doi:10.1029/2009JA014562
H. Volland, H.G. Mayr, Response of the thermospheric density to auroral heating during geomagnetic disturbances. J. Geophys. Res. **76**, 3764–3776 (1971)
Y. Wei, M. Hong, W. Wan, A. Du, J. Lei, B. Zhao, W. Wang, Z. Ren, X. Yue, Unusually long lasting multiple penetration of interplanetary electric field to equatorial ionosphere under oscillating IMF Bz. Geophys. Res. Lett. **35**, L02102 (2008). doi:10.1029/2008GL032305
Y. Wei, M. Hong, Z. Pu, Q.C. Zong, T. Nakai, X. Cao, J. Wang, S. Fu, L. Xie, J. Guo, X. Liu, Responses of the ionospheric electric field to a sheath region of iCME: a case study. J. Atmos. Sol.-Terr. Phys. **73**, 123–129 (2011). doi:10.1016/j.jastp.2010.03.004
R.A. Wolf, The quasi-static (slow flow) region of the magnetosphere, in *Solar Terrestrial Physics*, ed. by R. Carovillano, J.M. Forbes, D. Reidel (1983), pp. 303–380
Y. Yamazaki, M.J. Kosch, The equatorial electrojet during geomagnetic storm and substorms. J. Geophys. Res. Space Phys. **120**, 2276–2287 (2015). doi:10.1002/2014JA020773
K.Z. Zaka, A. Kobea, P. Assamoi, O.K. Obrou, V. Doumbia, K. Boka, B.J–P. Adohi, N.M. Mene, Latitudinal profile of the ionospheric disturbance dynamo magnetic signature; comparison with the DP2 magnetic disturbance. Ann. Geophys. **27**, 3523–3536 (2009)
K.Z. Zaka, A. Kobea, V. Doumbia, A.D. Richmond, A. Maute, N.M. Mene, O.K. Obrou, P. Assamoi, K. Boka, B.J–P. Adohi, C. Armory-Mazaudier, Simulation of electric field and current during the 11 June 1993 disturbance dynamo event: comparison with observations. J. Geophys. Res. **115** (2010). doi:10.1029/2010JA015417
Y. Zou, N. Nishitani, Study of mid-latitude ionospheric convection during quiet and disturbed periods using the SuperDARN Hokkaido radar. Adv. Space Res. **54**, 473–480 (2014). doi:10.1016/j.asr.2014.01.011

C. Xiong, H. Lühr, B.G. Fejer, The response of the equatorial electrojet, vertical plasma drifts, and thermospheric zonal wind to enhanced solar wind input. J. Geophys. Res. Space Phys. **121** (2016). doi:10.1002/2015JA022133